

Computational and Experimental Study on the Water-Jet Pump Performance

A. A. A. Sheha^{1†}, M. Nasr², M. A. Hosien³ and E. M. Wahba³

¹ Rotating Equipment Engineer, Petrogulfmiser Petroleum Company, 10, St. 250 Sarayat El-Maadi, Cairo, Egypt

² Dean of Alexandria Higher Institute of Engineering and Technology (AIET), Alexandria, Egypt

³ Mechanical Power Engineering Department, Faculty of Engineering, Menoufia University, Shebin El-Kom Egypt

†Corresponding Author Email: engineer_sheha@yahoo.com

(Received September 15, 2017; accepted January 13, 2018)

ABSTRACT

The effect of operational and geometrical parameters on the jet pump efficiency were determined experimentally and numerically. Numerical investigation was held firstly to determine the effect of diffuser angle, mixing chamber length, pump area ratio and driving nozzle position on the efficiency of jet pump. Commercial computational fluid dynamics (CFD) solver ANSYS FLUENT R 15.0 using SST-turbulence model was used. The numerical results showed that jet pump efficiency increases with decreasing both of diffuser angles and mixing chamber length up to a certain value and then pump efficiency decreases. Also, jet pump efficiency increases with increasing pump area ratio up to a certain value and then pump efficiency decreases. It was found that maximum numerical efficiency is 37.8 % for pump area ratio of 0.271. In addition, the numerical results showed that the optimum relative length of mixing chamber is 5.48 and the optimum value for diffuser angle at which the efficiency is a maximum value is 5°. Experimental tests were conducted to obtain the effects of various operational and geometrical parameters on the performance of the jet pumps. A test rig was constructed using the optimum design from the numerical results. The CFD's results were found to agree well with actual values obtained from the experimental results.

Keywords: Jet pump; CFD; Pump efficiency; Geometrical parameters; Operational parameters.

NOMENCLATURE

d	diameter	μ	dynamic viscosity
K	roughness height	ε	turbulent kinetic energy dissipation
k	turbulent kinetic energy	η	jet pump efficiency
l	length	ρ	fluid density
L	relative length of mixing chamber	$E_{\gamma 1}$	transition source
P	static pressure	$P_{\gamma 1}$	transition source
Re	Reynolds number	$E_{\gamma 2}$	destruction source
X	distance from the jet pump inlet	$P_{\gamma 2}$	relaminarization source
Z	relative position of driving nozzle	$P_{\theta t}$	source term
x_i	coordinate	\tilde{D}_k	destruction term for the turbulence model
x_n	driving nozzle position	\tilde{P}_k	production term for the turbulence model
M_r	flow rate ratio	Subscripts	
\dot{u}	fluctuation velocity component	d	discharge /outlet
ν	kinematic viscosity	n	nozzle
\dot{m}	mass flow rate	m	motive /primary fluid
P_r	pressure ratio	t	mixing pipe
ω	specific turbulent dissipation rate	s	suction, smooth
u_i	time-averaged velocity	dif.	diffuser
μ_t	turbulent viscosity		

1. INTRODUCTION

Jet pumps have come into widespread use in many branches of engineering. Jet pumps are simple

devices in terms of design, easy to fabricate and repair, perform reliably, do not require preliminary priming prior to start up, and permit the pumping of contaminated liquid. The efficiency of the jet pumps

are extremely affected by the geometrical and operational parameters of the jet pumps.

Schulz, F. (1952), Schulz, H. (1977) and Raabe, J. (1989) prepared a first design of the jet-pump in accordance with design guidelines.

Chamlong and Aoki (2002, August) developed a numerical investigation to the optimum mixing chamber length for driving nozzle position of the central jet pump. They investigated flow streamlines contours and the distribution of pressure along the pump with the change of position of the driving nozzle by 3D numerical investigation using Re-Normalization Group method (RNG) $k-\epsilon$ turbulent flow method. The results concluded that, when nozzle to mixing throat ratio (d_n/d_t) of jet pump is 0.6 the maximum efficiency is obtained.

Hammoud (2006) presented experimental observations for the performance of jet pump that deals with water using two suction types and designs. The results showed that, the optimum value for nozzle-to-throat spacing to nozzle diameter ratio is about 1.25 and the optimum value for motive fluid pressure is about 1.5 bar at a distance from the pump inlet (Z) of 1.25.

El-Sawaf *et al.* (2011) investigated experimentally the effect of area ratio, mixing chamber length, diffuser angle and nozzle to throat spacing on the jet pump performance with different flow rates and motive pressures. Their results illustrated that the optimum value for Z for pumping water is about 1.

Vyas and Kar (1972) generally suggested a method for the best design of the components of jet pump that deals with water and consequently for the all parts of pumping unit.

Teaima and Meakhail (2013) investigated experimentally and numerically the effects of driving pressure and the nozzle spacing on the pump performance. They concluded that the maximum efficiency of 25.6 % occurs at $Z = 0.5$ and the pumping liquid apt to cavitation as the nozzle to throat spacing is reduced to zero. They suggested a diffuser angle of 5.5° .

Aldas and Yapici (2014) carried out numerical study in order to determine the effect absolute and relative roughness on the jet pump efficiency. They conducted a study on a full-scale jet pump using four turbulence models the realizable $k-\epsilon$ model, Reynolds Stress Model (RSM-model), Menter's Shear Stress Transport (SST) $k-\omega$ model and transition Menter's Shear Stress Transport (SST) model. They compared all models results with the experimental results. The comparison illustrated that the transition SST model showed better reasonable results than other turbulence models.

Cunningham and Dopkin (1974) suggested an expression that an optimum throat length can be determined. They carried out several experiments to investigate the effect of changing nozzle shapes on pump efficiency. They recommended a mixing throat length of $6D_{th}$.

According to Prabkeao and Aoki (2005) the throat

length decreases as the nozzle-throat ratio increases. In addition the flow-ratio decreases as the mixing chamber length increases, when the nozzle location is closer to throat entrance.

Hansen and Kinnavy (1965) carried out experimental work to determine the optimum design parameters of water jet pumps. They found that the optimum value of x increases somewhat with area ratio.

El-Hayek and Hammoud (2006) presented a numerical investigation to predict the performance of liquid jet pumps. They used two turbulence models namely, the Reynolds stress model and the $k-\epsilon$ model. They concluded that the CFD techniques can be used in the field of jet pumps to illustrate the physics of the flow within the pump. The result showed the possibility of the improvement of the pump design.

Winoto *et al.* (2000) examined non-circular nozzles such as squared and triangular. Their results showed that all the examined configurations have lower efficiency compared to the circular shaped.

Zou *et al.* (2015) carried out numerical study in order to show the effect of horizontal installation and the vertical installation of the performance of jet pump. They used three turbulence models in order to calculate the flow field in the jet pump as a 3D single-phase flow. They compared the results with the experimental data to validate the numerical results. They concluded that the vertical inlet showed the highest efficiency.

Brijesh and Sagar (2016) carried out an experimental study to show the effect of change of diffuser angle on the jet pump performance. The experimental results showed that, changing the diffuser angle will affect jet pump behaviour. The maximum suction lift of the jet pump and the venturi of diffuser angle of 5° give the highest efficiency.

Xiaogang *et al.* (2017) investigated numerically the characteristics of the internal flow for both conventional and improved annular water-air jet pump. They concluded that the numerical comparison demonstrated an increase of approximately 10% pumping performance of improved annular water jet pump compared with the conventional pump.

It appears that there is a lack on the researches concerning studies on axial-water jet pumps using CFD, 2D techniques over a large range of design parameters. Therefore, the main purpose of the present numerical and experimental study is to investigate numerically the effects of the axial-water jet pump diffuser angle, area ratio, mixing chamber length and motive nozzle relative position on the pump performance using CFD simulation. A validation is held between the CFD, 2D results and the experimental results.

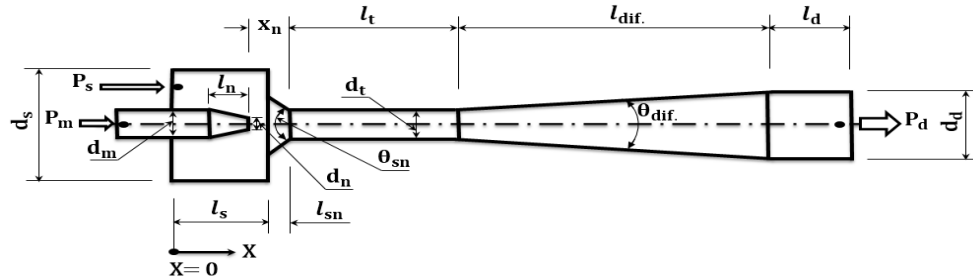
2. FLOW MODELLING IN JET PUMP

2.1 Physical Model

Axial-Jet pump is schematically shown in Fig. 1

with scale (1/1) and the main dimensions are given below the Figure. All cross sections at any part of pump is circular cross section. In the present study the inner surfaces of all parts of the pump assumed to be smooth surfaces ($K_s = 0.00015$ mm). As, all

pump parts are machined on the lath in a manner better than the new pipe. The 2D solid modelling different cases of the axial-jet pump with different dimensions were designed using Design Modeler software in an ANSYS Fluent R. 15.0.



l_s	d_s	l_{sn}	θ_{sn}	l_n	d_m	d_n	l_t	d_t	l_{dif}	θ_{dif}	l_d	d_d
110	152.4	25	86°	60	60	19	200	36.5	485	5°	100	80

All Dimensions are in (mm).

Fig. 1. Axial-jet pump geometry and dimensions with scale (1/1) at which the obtained maximum theoretical efficiency.

2.2 Numerical Model

The academic version of the ANSYS Fluent R 15.0 CFD code is used for all computations which employs a finite volume discretization. The 2D steady flow is used for numerical simulation of water flow through the used pump. The numerical simulation for the axial-water jet pump is held to study the effect of operational and geometrical parameters on axial-water jet pump and also to simulate flow behaviour through the pump under these different geometrical and operational parameters. In the current study, the transition SST model is suggested according to the recommendation of previous study; (Aldas and Yapici 2014). For a water jet pump the flow within it is a very complex flow. The following assumptions are made to analyse the water flow through the pump: (i) the flow is incompressible and steady flow. (ii) There is no heat transfer between surroundings and water, and (iii) ($K = 0$).

For incompressible flow the Reynolds-averaged continuity equation and momentum equation are as follows:

$$\frac{\partial(u_i)}{\partial x_i} = 0 \quad (1)$$

$$\rho \frac{\partial(u_i u_j)}{\partial x_j} = \frac{\partial}{\partial x_j} \left[\mu \frac{\partial u_i}{\partial x_j} \right] + \frac{\partial \tau_{ij}}{\partial x_j} - \frac{\partial P}{\partial x_i} \quad (2)$$

Where; the Reynolds stress is:

$$\tau_{ij} = -\rho u_i u_j = \mu_t \left[\frac{\partial u_i}{\partial x_j} + \frac{\partial u_j}{\partial x_i} \right] - \frac{2}{3} k \rho \delta_{ij} \quad (3)$$

The transition SST model is about four equation turbulence model. The four equations are illustrated as below. The intermittency (γ) transport equation is:

$$\frac{\partial(\rho \gamma)}{\partial t} + \frac{\partial(\rho u_j \gamma)}{\partial x_j} = -E_{\gamma 1} + P_{\gamma 1} - E_{\gamma 2} + P_{\gamma 2} +$$

$$\frac{\partial}{\partial x_j} \left[\left(\mu + \frac{\mu_t}{\sigma_\gamma} \right) \frac{\partial \gamma}{\partial x_j} \right] \quad (4)$$

The transition momentum thickness transport equation that illustrates transition onset criteria is:

$$\frac{\partial(\rho \tilde{R}e_{\theta t})}{\partial t} + \frac{\partial(\rho u_j \tilde{R}e_{\theta t})}{\partial x_j} = P_{\theta t} + \frac{\partial}{\partial x_j} \left[\sigma_{\theta t} (\mu + \mu_t) \frac{\partial \tilde{R}e_{\theta t}}{\partial x_j} \right] \quad (5)$$

The transport equation for turbulence kinetic energy (k) is:

$$\frac{\partial}{\partial x_j} (\rho u_j k) = -\tilde{D}_k + \gamma_{eff} \tilde{P}_k + \frac{\partial}{\partial x_j} \left[(\mu + \sigma_k \mu_t) \frac{\partial k}{\partial x_j} \right] \quad (6)$$

The transition SST Model details can be obtained from (Langtry *et al.* 2004) and (Menter *et al.* 2004 and 2006).

A half of the pump is used as the computational domain in the simulation without using the whole pump due to the rotational symmetry of the axial-jet pump. The number of cells used in the current study to obtain mesh independent solutions are 21209. Mesh inflation is used beside non-straight walls.

3. EXPERIMENTAL TEST RIG

The experimental work in the present study is carried out to provide experimental data for extensive model validation and optimum model verification. This is achieved by constructing a test rig including axial-water jet pump test model in the Fluid Mechanics Laboratory of the Mechanical Power

Engineering Department, Faculty of Engineering, Minoufia University, Egypt. The principal objective of this work is to study the effect of the major controlling parameters that have direct effects on the axial jet pump performance. These parameters are the inflow motive pressure and nozzle spacing.

The experimental test rig schematic diagram is shown in Fig. 2. The test rig consists of three

tanks, orifice meter, centrifugal pump, jet pump, pressure gages, u-tube manometer, multi-tube manometer and piping system.

The test rig including axial jet pump test model was held in a manner that enabling change nozzle relative position of jet pump. The present experimental test rig was modified three times in order to obtain three relative positions of a values of $Z = 0, 1$ and 2 .

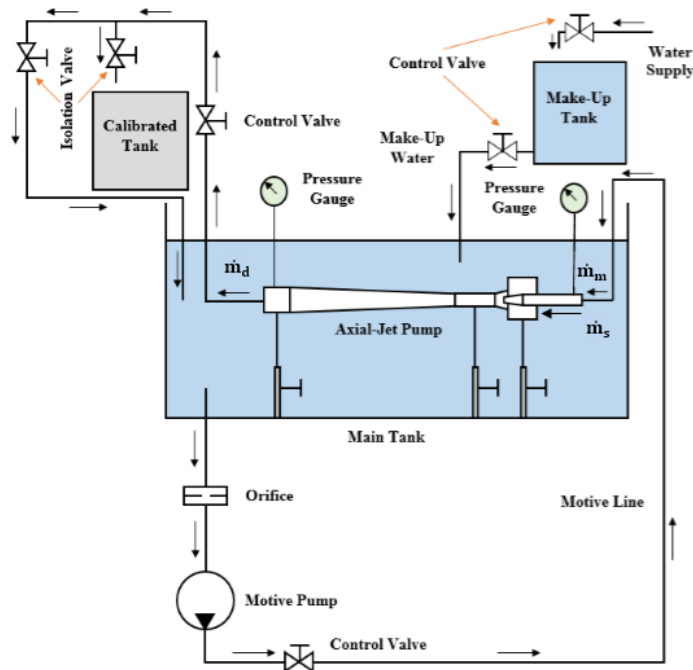


Fig. 2. Schematic diagram of the experimental test rig.

The parameters that describe the performance of jet pumps are defined as follows:

(i) Mass Flow Ratio (M_r)

The mass flow ratio can be represented as the following:

$$M_r = \frac{\dot{m}_s}{\dot{m}_m} \quad (7)$$

(ii) Pressure Ratio (P_r)

The pressure ratio can be represented as the following:

$$P_r = \frac{(P_d - P_s)}{(P_m - P_d)} \quad (8)$$

(iii) Efficiency (η)

The jet pump efficiency can be obtained by multiplying mass flow ratio by pressure ratio.

$$\eta = M_r \cdot P_r \quad (9)$$

In this simulation study, validation was held between CFD, 2D present results and (experimental – CFD, 3D) data (Aldas and Yapici 2014) at the same 1/1-scale jet pump dimensions. Figures 3-(a and b) shows the experimental and numerical

results of the pump efficiency and pressure ratio with mass flow ratio. Figure (3-a) illustrates that the pump efficiency increases, showing a peak at about $M_r = 1.7$ and then decreases with increasing mass flow rate ratio.

Figure (3-b) shows that the pressure ratio in jet pump and it decreases nearly linearly with the mass flow ratio increase. In addition, the present 2D numerical results are relatively in close agreement with the experimental and 3 D numerical results obtained by (Aldas and Yapici 2014) in the region of mass flow ratio up to 1.7. However, for mass flow ratio more than 1.7 the present 2D numerical results gives higher efficiency than those of (Aldas and Yapici 2014). Moreover, Fig. 3 shows that the numerical 2D results using the turbulence model (SST) shows a reasonable agreement with experimental results and numerical 3D results using the same turbulence model. Therefore, CFD, 2D technique is used in this investigation which saves computational time and cost. Also, it helps in saving efforts exerted in laboratories in order to predict one or more geometrical and operational parameters.

The variations of the pressure and velocity across the centreline of the pump with the distance from

the pump inlet at the same 1/1 scale pump are shown in Figs. 4-(a and b). As shown in Fig. (4-a), the negative pressure value a long suction chamber exit, suction nozzle and mixing chamber did not reach to the value of water vapor pressure at the operating temperature. In addition, the jet pump is

submersed in the main tank as seen in Fig. 2.

Figure 4 shows the results of present numerical 2D and numerical 3D data (Aldas and Yapici 2014). Uncertainty analysis should be conducted on all data collected from all measurements in order to

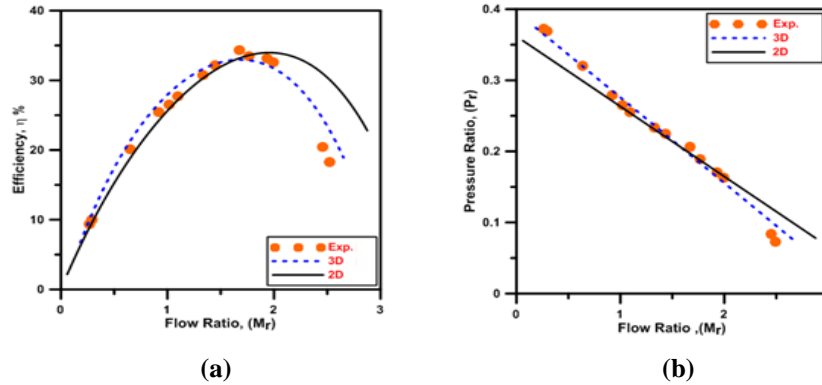


Fig. 3. Comparison between the present CFD, 2D results and (experimental – CFD, 3D) data (Aldas and Yapici 2014).

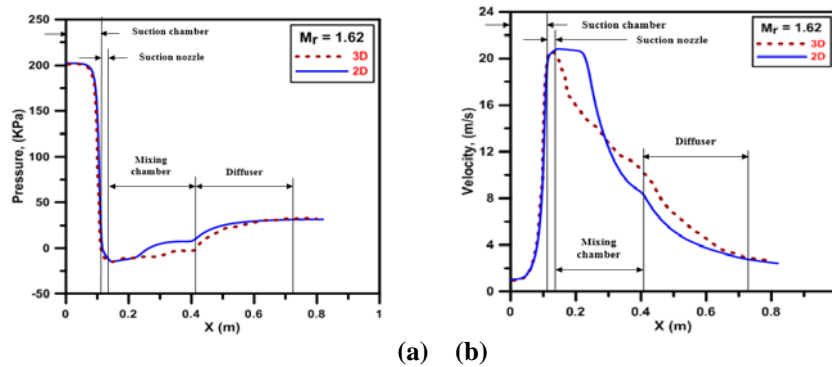


Fig. 4. Comparison between the present numerical, 2D results and numerical, 3D data (Aldas and Yapici 2014).

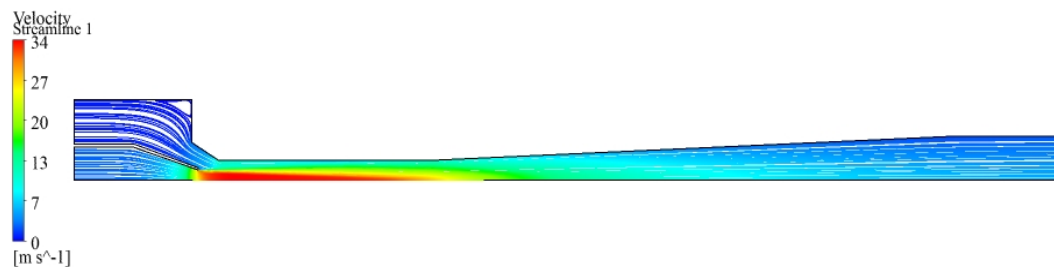


Fig. 5. Velocity distribution and streamlines at mass flow ratio ($M_r=1.19$) for scale (1/1) jet pump at which the obtained maximum theoretical efficiency ($A_r = 0.271$).

quantify the data and validate the accuracy, see Table 1.

4. RESULTS AND DISCUSSION

The comparison between experimental results and numerical results are illustrated and discussed in this section. The comparisons are conducted at the

same geometries and the same operating conditions.

4.1 Velocity Distribution and Streamlines

As shown in Fig. 5. The velocity of motive flow decreases gradually and the velocity of the entrained water increases along the mixing chamber at the same time due to the jet from the motive nozzle. Therefore, the motive flow kinetic energy that way out from motive nozzle is shifted to the

Table 1 Uncertainty for performance parameters of the axial-water jet pump.

Parameter	Percentage uncertainty ($\pm \%$)	
	Min. uncertainty	Max. uncertainty
Total discharge of jet pump (Q_t)	0.571	1.01
Motive discharge for jet pump (Q_m)	0.613	1.12
Efficiency of jet pump	0.145	0.698

entrained fluid and energy losses in this case are nearly neglected. Consequently, the efficiency of jet pump reaches to a maximum value at this flow rate ratio.

As shown in Figs. 6-(a and b), the pressure and velocity distribution along the centerline of the jet pump are shown. At the lower flow rate ratio $M_r = 0.16$, the liquid pressure rises sharply at slightly ahead of the mixing chamber inlet, due to a higher back (exit) pressure acting on the pump. So, the mass flow rate of the entrained liquid drops due to the previous flow behavior. Despite the inlet pressures for the pump differ for both of lower and higher flow rate ratios, the pressure value for the optimum flow ratio is higher than the pressure for the higher flow ratio along suction chamber. As shown in Fig. (6-a) the pressure for the optimum flow ratio drops to a value lower than the pressure for the higher flow ratio along the suction nozzle and mixing chamber inlet and then increases suddenly along the mixing chamber exit and diffuser. The trends of velocity variation and pressure variation along the centerline of the pump are opposite, as shown in Figs. 6-(a and b).

4.2 Jet Pump Wall Pressure Distribution

A comparison between experimental and theoretical results generated by the commercial software, the ANSYS R 15.0 FLUENT at the same geometries and the same operating conditions is carried out. The experimental test pump here is manufactured using the optimum mixing chamber relative length ($L = 5.48$), the optimum angle of diffuser of ($\theta_{dif} = 5^\circ$) and area ratio (Motive nozzle outlet area / Mixing chamber area) of $A_r = A_n / A_t = 0.271$ at which the obtained maximum numerical efficiency.

Figures 7-(a, b and c), show the measured experimental pressure values along the outer wall of jet pump experimental test model and theoretical pressure values calculated numerically at various flow ratios ranged from 0.035 to 1.9 with the same nozzle relative position of $Z = 0, 1$ and 2. The comparison shows good agreement between the results obtained experimentally and numerically along the mixing chamber section. Also, in the diffuser section the agreement between experimental and numerical results is fair for higher mass flow ratios. Unfortunately, the agreement is to

some extent weak at lower mass flow ratios for all the used values of the relative positions (Z).

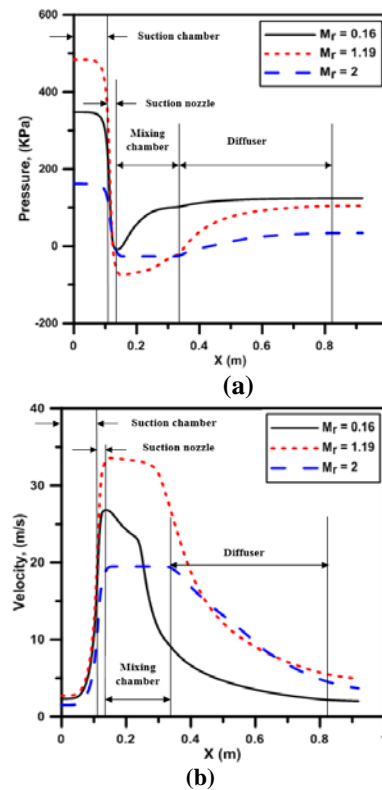
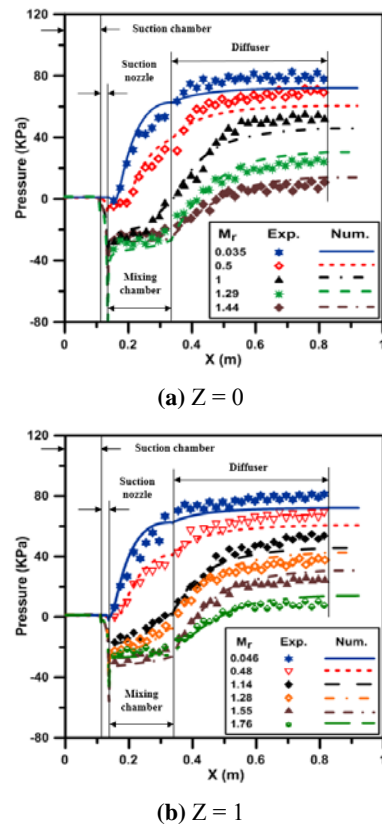
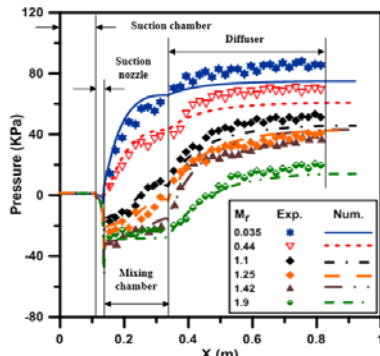


Fig. 6. Pressure (a) and velocity (b) variations along centreline of jet pump.





(c) $Z = 2$

Fig. 7. (a, b and c) Comparison between experimental and numerical pressure variations along the outer wall of jet pump.

4.3 Comparison Between Experimental and Numerical Efficiency and Head Ratio Curve

Comparison between experimental and numerical results of both the efficiency and head ratio at various flow ratios with different relative positions of 0, 1, and 2 are given in Figs. 8 and 9 respectively. The comparison between the experimental and numerical values is in good agreement.

Either experimental results or numerical results showed that the lowest efficiency at the smallest nozzle relative position of ($Z = 0$), and the highest value of efficiency at ($Z = 1$), as seen in Fig. 8. In addition the position of the maximum efficiency is shifted to the right at increasing the relative position of nozzle.

Figure 9 shows the experimental and numerical results of the variation of pressure ratio with mass flow ratio at different nozzle relative positions. This

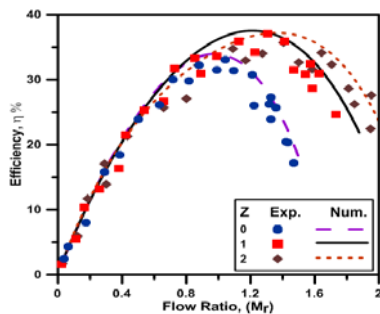


Fig. 8. Comparison between experimental and numerical data for the three relative positions; efficiency curve.

REFERENCES

Aldas, K. and R. Yapici (2014). Investigation of Effects of Scale and Surface Roughness on Efficiency of Water Jet Pumps Using CFD. *Engineering Applications of Computational Fluid Mechanics* 8(1), 14–25.

Brijesh, R. N. and M. P. Sagar (2016, June). The

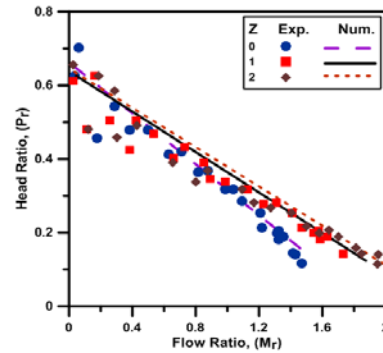


Fig. 9. Comparison between experimental and numerical data for the three relative positions; head ratio curve.

Figure shows that the head ratio decreases nearly linearly with increasing mass flow ratio larger than 0.4.

5. CONCLUSIONS

The important conclusions that can be drawn are as follows:

1. In the current numerical study, thirty five different axial-water jet pumps having diffuser angles ranging from 2.5° to 9° , relative lengths of mixing chamber ranging from 3.32 to 7.4 and area ratios ranging from 0.108 to 0.331 were carried out using the transition SST turbulence model in 2D technique.
2. For the purpose of validation, the numerical 2D results were compared with the optimized experimental results and 3D results at the same geometry and boundary conditions in the literature. The numerical, 2D results relative to the experimental results and numerical, 3D results showed a reasonable agreement
3. The numerical results obtained showed that the optimum value for diffuser angle at which the efficiency is a maximum value is 5° . Furthermore, the optimum relative length of mixing chamber is ($L = 5.48$).
4. The highest efficiency of 37.8 % was determined by transition SST turbulence model for the area ratio of ($A_r = 0.271$), mixing chamber relative length ($L = 5.48$), diffuser angle ($\theta_{dif} = 5^\circ$), relative position of the nozzle ($Z = 1$), flow ratio of ($M_r = 1.19$), and pressure ratio of ($P_r = 0.317$).

Effect of Venturi Design on Jet Pump Performance. *Journal for Research* 2(4), 23-28.

Chamlong, P. and K. Aoki (2002, August). Numerical Prediction on the Optimum Mixing Throat Length for Drive Nozzle Position of the Central Jet Pump. *Proceedings of Tenth international symposium on flow visualization*, 26-29, Kyoto, Japan.

- Cunningham, R. G. and R. J. Dopkin (1974). Jet Breakup and Mixing Throat Lengths for the Liquid Jet Gas Pump. *J. Fluid Engineering, Trans. ASME*, 93(3), 216–226.
- El Hayek, M. D. and A. H. Hammoud (2006, August). Prediction of Liquid Jet Pump Performance Using Computational Fluid Dynamics. *Proceedings of the 4th WSEAS International Conference on Fluid Mechanics and Aerodynamics*, Elounda, Greece, 21-23, 148-153.
- El-Sawaf, I. A., M. A. Halawa, M. A. Younes, and I. R. Teaima (2011). Study of the Different Parameters That Influence on the Performance of Water Jet Pump. *Fifteenth International Water Technology Conference, IWTC 15*, Alexandria, Egypt.
- Hammoud, A. H. (2006, August). Effect of Design and Operational Parameters on Jet Pump Performance. *Proceedings of the 4th WSEAS International Conference on Fluid Mechanics and Aerodynamics*, Elounda, Greece, 21-23, 245-252.
- Hansen, A. G., and R. Kinnavy (1965) The design of water jet pumps Part-I- Experimental determination of optimum design parameters. *ASME paper*, 65-WA/FE-31.
- Langtry, R. B., F. R. Menter, S. R. Likki, Y. B. Suzen, P. G. Huang and S. Völker, (2004, June) A correlation-Based Transition Model Using Local Variables, Part -2-Test Cases and Industrial Applications. *In Proceedings of the ASME Turbo Expo*. Vienna, Austria, 14-17, paper no. GT2004-53454.
- Menter, F. R., R. B. Langtry, and S. Völker (2006). Transition Modeling for General Purpose CFD Codes. *Flow Turbul. Combust.* 77(1–4): 277–303.
- Menter, F. R., R. B. Langtry, S. R. Likki, Y. B. Suzen, P. G. Huang, and S. Völker, (2004, June). A Correlation Based Transition Model Using Local Variables, Part-1- Model Formulation. *In Proceedings of the ASME Turbo Expo*. Vienna, Austria, 14–17, paper no. GT2004–53452.
- Prabkeao, C. and K. Aoki (2005). Study on the Optimum Mixing Throat Length for Drive Nozzle Position of the Central Jet Pump. *Journal of Visualization*, 8(4), 347–355.
- Raabe, J. (1989). *Hydraulische Maschinen und Anlagen*. VDI Verlag.
- Schulz, F. (1952). *Modellversuche für Wasserstrahl- Wasserpumpen*. *Habil. TU*, Wien.
- Schulz, H. (1977). *Die Pumpen*. Springer Verlag.
- Teaima, I. R. and T. A. Meakhail (2013, September). A Study of the Effect of Nozzle Spacing and Driving Pressure on the Water Jet Pump Performance. *International Journal of Engineering Science and Innovative Technology (IJESIT)* 2(5).
- Vyas, B. D. and S. Kar (1972). Standardization of water jet pumps. *Proc., Symp. on jet Pumps and ejectors*, paper 10, London, U.K., PP. 155-170.
- Winoto, S. H., H. Li, and D. A. Shah (2000). Efficiency of Jet Pumps. *Journal of Hydraulic Engineering*, 126(2):150–156.
- Xiaogang, D., D. Jingliang, W. Zhentao, and T. Jiyuan (2017). Numerical analysis of an annular water–air jet pump with self-induced oscillation mixing chamber. *The Journal of Computational Multiphase Flows*, pp. 1-7.
- Zou, C. H., H. Li. P. Tang and D. H. Xu (2015). Effect of structural forms on the performance of a jet pump for a deep well jet pump. *National Research Center of Pumps and Pumping System Engineering and Technology*, Jiangsu University, China, 59, 257-266.